Contents lists available at ScienceDirect

Current Research in Microbial Sciences

The core Cas1 protein of CRISPR-Cas I-B in *Leptospira* shows metal-tunable nuclease activity

Bhuvan Dixit, Formal analysis Writing – original draft [a], Aman Prakash, Formal analysis [a], Pankaj Kumar, Formal analysisWriting – original draft [b], Prerana Gogoi, Writing – original draft [a], Manish Kumar, Conceptualization Supervision Formal analysisWriting – original draft [a,*]

[a] *Department of Biosciences and Bioengineering, Indian Institute of Technology Guwahati, Guwahati, Assam 781039, India*
[b] *Division of Livestock and Fisheries Management, ICAR Research Complex for Eastern Region, Patna, Bihar 800014, India*

A B S T R A C T

Leptospira interrogans serovar Copenhageni strain Fiocruz L1-130 is the causative agent of leptospirosis in animals and humans. This organism carries a functional *cas1* gene classified under CRISPR-Cas I-B. In this study, using various nuclease assays and bioinformatics analysis, we report that the recombinant Cas1 (LinCas1) possesses metal-ion dependent DNase activity, which is inhibited upon substitution or chelation of metal-ion and/or interaction with recombinant Cas2 (LinCas2) of *L. interrogans*. Model of LinCas1 structure shows a shorter N-terminal domain unlike other Cas1 orthologs reported to date. The C-terminal domain of LinCas1 contains conserved divalent-metal binding residues (Glu108, His176, and Glu191) and the mutation of these residues leads to abolition in DNase activity. Immunoassay using anti-LinCas2 demonstrates that LinCas1 interacts with LinCas2 and attains a saturation point. Moreover, the nuclease activity of the LinCas1-Cas2 mixture on ds-DNA displayed a reduction in activity compared to the pure core LinCas proteins under *in vitro* condition. The DNase activity for LinCas1 is consistent with a role for this protein in the recognition/cleavage of foreign DNA and integration of foreign DNA as spacer into the CRISPR array.

1. Introduction

CRISPR-Cas (Clustered Regularly Interspaced Short Palindromic Repeats- CRISPR associated proteins) is an emerging microbial acquired immune defense system against the foreign genetic elements transferred horizontally from viruses and plasmids (Barrangou et al., 2007; Yosef et al., 2012; Heler et al., 2014). The CRISPR-Cas systems have been classified into six major types (Type I-VI). Each type is further sub-divided into various subtypes based on signature cas genes and the locus arrangement (Makarova et al., 2015; Koonin et al., 2017). The architecture of the CRISPR-Cas immune system comprises of an array of palindromic direct repeats interrupted by the variable spacers and a set of associated *cas* genes (Haft et al., 2005; Pourcel et al., 2005; Garneau et al., 2010; Makarova et al., 2015). AT-rich regions precede the first direct repeat called a leader sequence (Yosef et al., 2012; Sternberg et al., 2016). CRISPR immunity is initiated by acquiring the foreign genetic material into CRISPR arrays (Westra et al., 2012). The two core proteins Cas1 and Cas2 obtains short foreign DNA fragments

(protospacers) from the invasive genetic element and integrates them into the CRISPR array as new spacers between the leader end and the start of the first repeat (Makarova et al., 2015; Koonin et al., 2017). Protospacer-adjacent motifs (PAMs) in the DNA of invasive genetic elements determine the acquisition efficiency and integration specificity during the spacer acquisition process (Bolotin et al., 2005; Deveau et al., 2008; Mojica et al., 2009). The Cas1-Cas2 complex processes the acquired protospacers by cleaving-off the PAM sequence to appropriate sizes before integrating it into the CRISPR array (Yosef et al., 2012; Nuñez et al., 2014; Levy et al., 2015; Nuñez et al., 2015; Wang et al., 2015; Xiao et al., 2017; He et al., 2018; Kieper et al., 2018; Rollie et al., 2018). Among diverse CRISPR-Cas systems, the PAM dependent spacer acquisition is observed only in type-I, -II and -V (Bolotin et al., 2005; Deveau et al., 2008; Mojica et al., 2009; Shah et al., 2013; Heler et al., 2014). Bioinformatics and various enzymatic assays describe Cas1 to function as a nuclease/integrase (Makarova et al., 2006). Cas1 is a metal-dependent nuclease that can cleave a range of different substrates, including single-stranded DNA (ss-DNA), double-stranded DNA

(ds-DNA), branched DNA, and plasmid DNA (Wiedenheft et al., 2009; Babu et al., 2011; He et al., 2018). Two types of phosphodiester bonds, 5′ or 3′ of a scissile phosphate, can be cleaved in DNA by the nucleases through nucleophilic substitution. The metal-ion-dependent phosphodiester hydrolysis of DNA involves metal-ion in nucleophile activation, transition state stabilization, and leaving group protonation (Dupureur, 2008; Yang, 2011).

The previous sequence analysis of Cas1 described elsewhere (Makarova et al., 2002) stipulates that four strictly conserved residues (three carboxylates and one histidine) represent the signature motif of the Cas1 family. To date, Cas1 proteins from six different bacteria and one phage have been crystallized (Babu et al., 2011; Wiedenheft et al., 2012; Kim et al., 2013; Ka et al., 2016; Wilkinson et al., 2016; Yang et al., 2020). The crystal structures of Cas1 proteins show it to exist in the homo-dimeric state whose monomer is organised into an N-terminal β-strand domain (NTD) and a C-terminal α-helical domain (CTD) connected by a small linker. However, the catalytic residues responsible for the hydrolysis of nucleic acid are existing within the CTD, whereas the NTD interact with adjacent protomers to promote a stable Cas1 homo-dimer state (Wiedenheft et al., 2009; Kim et al., 2013; Nuñez

et al., 2014; Ka et al., 2016; Wilkinson et al., 2016). Nevertheless, from the structural point of view, the Cas1 nuclease activity observed against different substrates has failed to provide significant insights into substrate specificity except that of *E. coli* Cas1-Cas2 (Wang et al., 2015). Therefore, further detailed enzymatic studies of Cas1 proteins from diverse organisms are required to delineate the functional versatility of this nuclease family.

The pathogenic and intermediate strains of *Leptospira* that cause leptospirosis disease in animals and human possess three subtypes (I-B, I-C, and I-E) of the CRISPR-Cas system whereas, type V CRISPR-Cas system has been recently reported in the saprophytic strain of *Leptospira* (*L. biflexa*) (Makarova et al., 2011; Xiao et al., 2019; Arbas et al., 2021). In a recent computational study, a weakly conserved PAM sequence (5′-TAC-3′) has been predicted for CRISPR-Cas I-B of *Leptospira* (Xiao et al., 2019). Bioinformatics and transcriptional analysis have revealed that CRISPR-Cas I-B exists in the *L. interrogans* genome, wherein a functional *cas1* gene has previously been disclosed to be transcriptionally active (Dixit et al., 2016). As part of our ongoing investigation of the CRISPR-Cas I-B system in *Leptospira* (Dixit et al., 2021; Prakash and Kumar, 2021), in this study, we explored the nuclease activity of
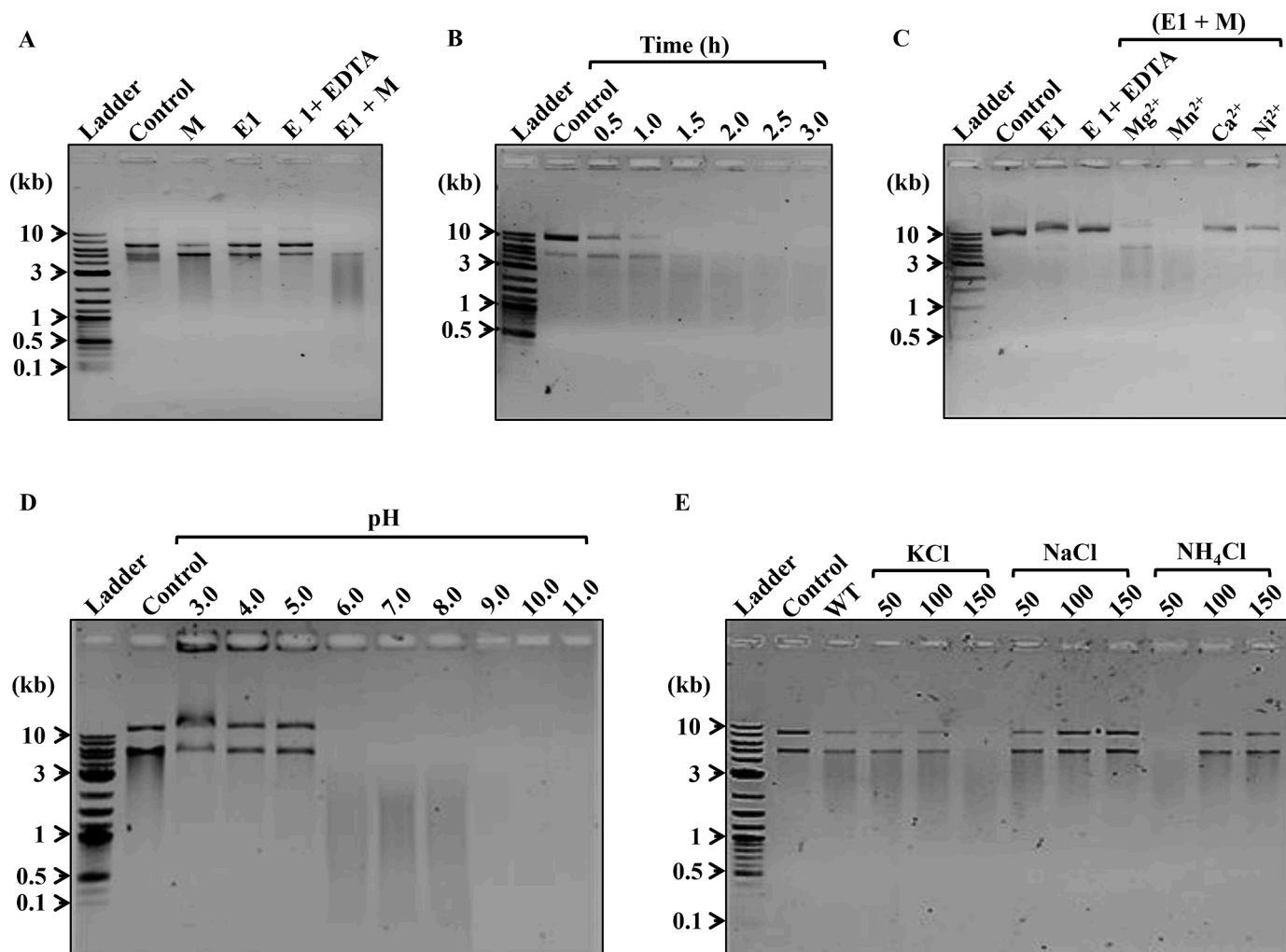

Fig. 1. LinCas1 nuclease activity on double-stranded DNA. In all panels, E1 represents LinCas1 and M denotes Mn^{2+}. All the reactions were carried out for 1 h at 37 °C unless stated. (A) LinCas1 shows metal-ion dependent DNase activity. LinCas1 activity on plasmid DNA (pTZ57R/T; 2.9 kbp) in the presence or absence of metal-ion. EDTA was used as a metal-ion chelator in the absence of Mn^{2+} ion to rule out the presence of any metal-ion that may have co-purified. (B) Time-dependent DNase activity in LinCas1. Nuclease activity on plasmid DNA (pTZ57R/T) as substrate (1 μg) was performed for the different duration (0.5–3 h) where LinCas1 shows complete cleavage of DNA in 2.5 h. (C) LinCas1 DNase activity in the presence of different divalent-metal illustrates its preference for Mn^{2+}. (D) Nuclease activity in LinCas1 on ds-DNA at different pH. DNase activity in LinCas1 is exhibited at pH 6.0–11.0 and is best observed at pH 9.0–11.0. (E) Effect of different monovalent ions and its varying concentrations on LinCas1 ds-DNase activity. The DNA cleavage reaction shows that 150 mM of KCl or 50 mM of NH_4Cl are optimal for LinCas1 activity on DNA. WT indicates nuclease activity without any monovalent ions. Results presented were confirmed by two independent experiments.

recombinant Cas1 protein (LinCas1) and its mutant variants. In this study, we intend to show that LinCas1 possesses metal-ion dependent DNase activity, which is inhibited upon substitution of metal-ion or its binding residues. The nuclease and immunoassay demonstrate that LinCas1 interacts with LinCas2 and the mixture of LinCas1-Cas2 shows restrained nuclease activity than the pure core Cas proteins.

2. Results

2.1. Leptospira Cas1 nuclease activity on double-stranded DNA

The recombinant LinCas1 was purified using Ni-affinity chromatography with a yield of 0.3 mg/L (Fig. S1A and B). The yield and concentration of LinCas1 could not be further improvised even after performing multiple attempts of overexpression and purification of LinCas1 in numerous expression vectors. Nuclease assay performed with the given LinCas1 concentration (6 μM) manifested metal-ion (Mn^{2+}) dependent endo-deoxyribonuclease activity against circular ds-DNA (pTZ57R/T vector) where the substrate (1 μg) was completely cleaved in 2.5 h (Fig. 1A and B). The Cas1 has been reported to recognize the proximal PAM sequence in the protospacer bound by the Cas1-Cas2 complex and trims the protospacer at the PAM before its integration in the CRISPR loci (Yosef et al., 2012; Nuñez et al., 2014,2015; Levy et al., 2015; Wang et al., 2015; Xiao et al., 2017; He et al., 2018; Kieper et al., 2018; Rollie et al., 2018). Based on this, we investigated if the cleavage of the circular ds-DNA by the LinCas1 is driven by the presence of a possible PAM motif in the pTZ57R/T vector. The vector sequence was derived from the SnapGene tool for screening the PAM motif. In the pTZ57R/T nucleotide sequence, around 60 PAM motifs (5′-TAC-3′) were determined, perhaps that may be recognized by the LinCas1 during cleavage. The determination of the number of PAM motifs (5′-TAC-3′) was based on a lead from a recent study about PAM in *L. interrogans* (Xiao et al., 2019). For studying metallonucleases, substituting metal-ions is a common practice to understand the role of metal-ions in the nuclease activity. On replacing Mn^{2+} with other divalent metals (Mg^{2+}, Ca^{2+}, and Ni^{2+}), we observed that LinCas1 prefers Mn^{2+} followed by Mg^{2+} for DNase activity. In the presence of Ni^{2+} or Ca^{2+}, the DNase activity of LinCas1 gets equally reduced (Fig. 1C). The endonuclease activity in LinCas1 is inhibited by EDTA due to the chelation of the divalent-metal (Fig. 1C). Upon heat inactivation of LinCas1 at 100 °C for 10 min, the DNase activity was observed to be abrogated entirely, and a shift in the mobility of the circular ds-DNA was noticed (Fig. S2).

Next, the effect of pH (pH 3.0–11.0) in LinCas1 nuclease activity on ds-DNA was studied as described previously for LinCas2 and LinCas4 (Dixit et al., 2016,2021). The nuclease activity of LinCas1 was inhibited below pH 6.0. (Fig. 1D). At pH 3.0, no smear of DNA cleavage products was evident, suggesting the abolition of nuclease activity. Moreover, at pH 3-5, due to nucleo-protein interaction, a shift in the migration of a fraction of DNA substrate was exhibited on agarose gel electrophoresis (Fig. 1D). LinCas1 exhibited maximum nuclease activity at a wide pH range (pH 6–11). Thereafter all the nuclease assays were preferred to be done in the range of pH 7-7.5. The effect of salt on endonuclease activity in LinCas1 in the presence of Mn^{2+} was analyzed by using various monovalent-ions (NaCl, KCl, and NH_4Cl) at an increasing concentration (Fig. 1E). LinCas1 optimum endonuclease activity on ds-DNA was observed at 150 mM of KCl or 50 mM NH_4Cl (Fig. 1E). However, in the presence of NaCl (50–150 mM), LinCas1 did not exhibit a considerable endonuclease activity (Fig. 1E). To understand the diversity of nuclease activity in LinCas1, substrates other than ds-DNA were used in nuclease assays. LinCas1 cleaves viral single-stranded DNA (linear M13mp18 and circular φx174) only in the presence of divalent-metal cofactor (Fig. 2A and B). Interestingly, LinCas1 did not demonstrate any cleavage activity on shorter DNA oligos (28 and 37-mer nucleotides) (Fig. 2C). The inability of the LinCas1 to cleave the short oligos may have been due to the absence of the probable PAM sequence (5′-TAC-3′) of *L. interrogans* type I-B CRISPR-Cas system or is substrate size-dependent.

2.2. In silico characterization of Cas1 protein

A homology search for LinCas1 revealed its closest homologs to be Cas1 protein from thermophilic organisms, including *Thermotoga maritima* (sequence identity: 28% and query coverage: 96%), *Aquifex aeolicus* (27 and 95%) and *Archaeoglobus fulgidus* (27 and 79%). Low sequence similarity was observed for Cas1 protein from other organisms with solved crystal structures such as *Streptococcus pyogenes* (23 and 55%) and *Escherichia coli* (36 and 35%). The least sequence similarity was perceived for Cas1 proteins from *Pectobacterium atrosepticum* (67 and 6%) and *Pseudomonas aeruginosa* (67 and 2%). A multiple sequence alignment (MSA) was performed to identify the conserved residues in LinCas1 with the crystallized Cas1 proteins from different organisms. Though Cas1 orthologs showed a more extensive range of sequence similarity, the amino acid residues involved in metal-ion binding was highly conserved in all the Cas1 orthologs (Fig. 3). Notably, the LinCas1 (Lin) also possesses all the conserved metal-ion interacting residues (Glu108, His176, and Glu191) located at the CTD (Fig. 3). Moreover, the residues Asn145 and Asp188 present in the vicinity of the metal-ion
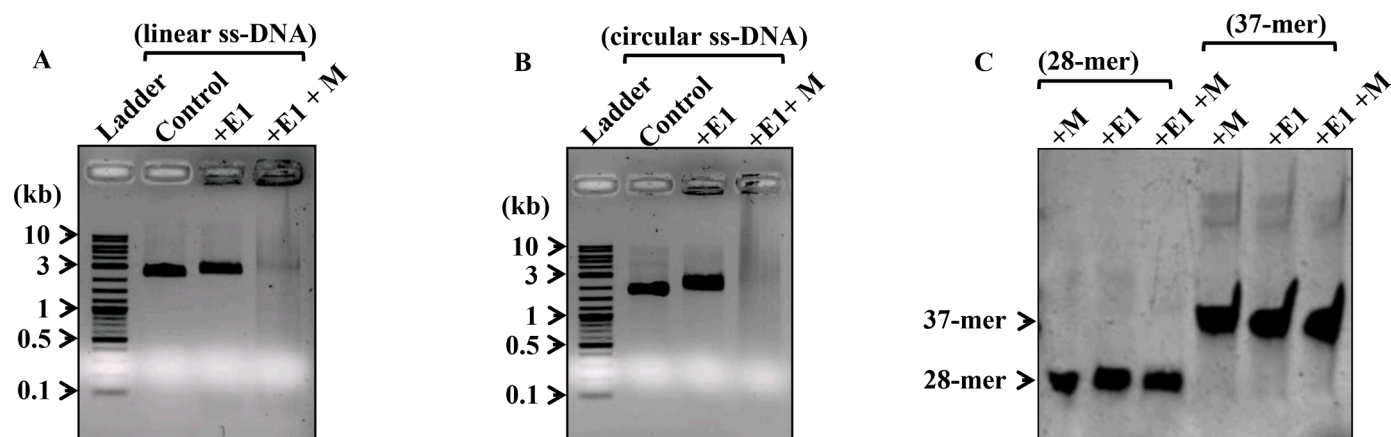

Fig. 2. LinCas1 nuclease activity on single-stranded DNA. In all panels, E1 represents LinCas1, and M denotes Mn^{2+}. All the reactions were carried out for 1 h at 37 °C unless stated. (A) Nuclease activity in LinCas1 on linear ss-DNA (M13mp18 vector; 7.2 kb) shows that Mn^{2+} ion is required for cleaving linear ss-DNA. (B) Nuclease activity in LinCas1 on circular ss-DNA (φx174 genome; 5.3 kb) shows that Mn^{2+} ion is required for cleaving circular ss-DNA. (C) LinCas1 activity on short DNA oligos. Oligonucleotides of 28-mer and 37-mer were used as the substrate for nuclease activity and the reaction product was resolved on 18% Urea PAGE. No activity on short oligonucleotides was observed in the presence or absence of metal-ions. Results presented were confirmed by two independent experiments.
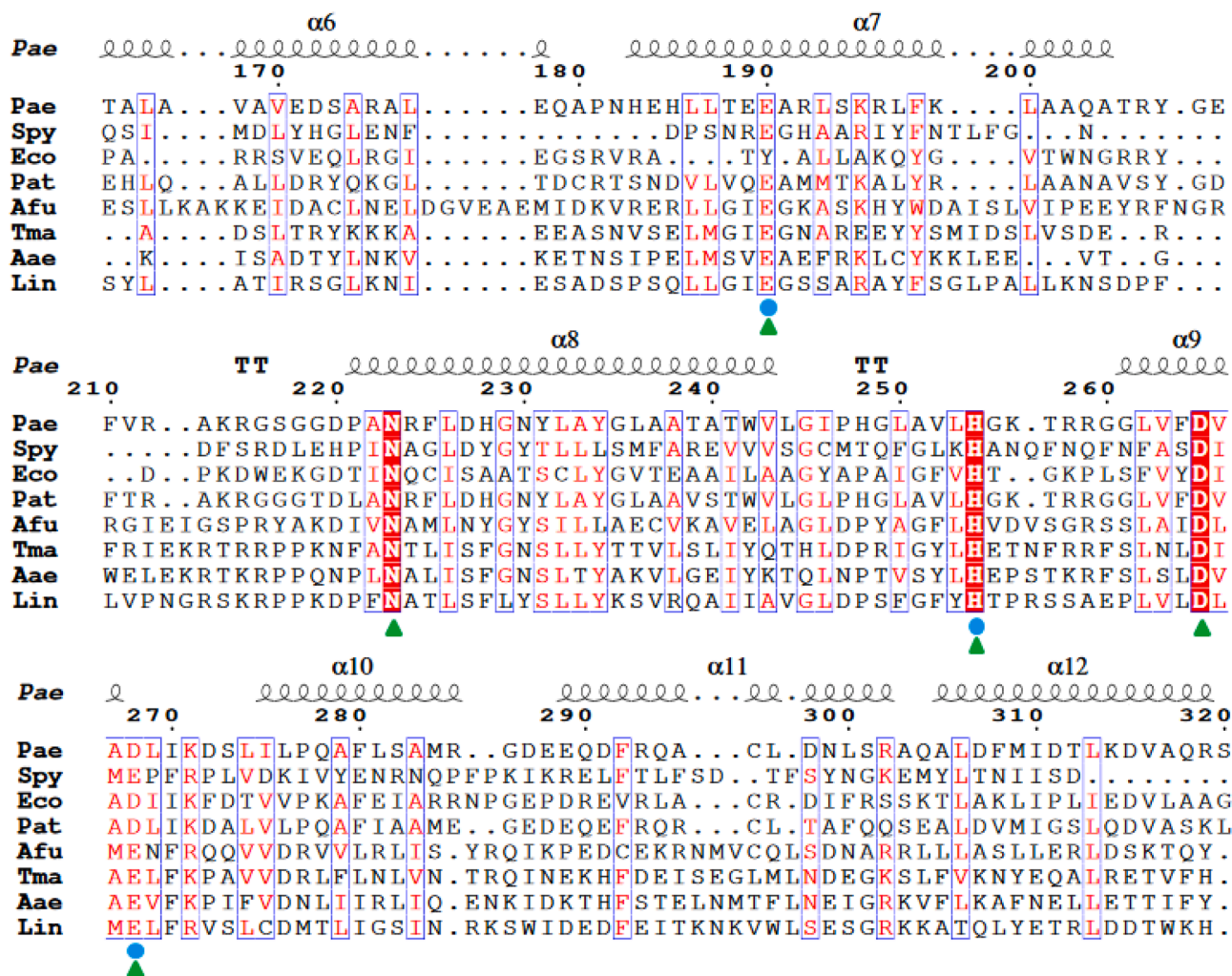
α6 α7
Pae   170   180   190   200

Pae TALA...VAVEDSARAL......EQAPNHEHLLTEEARLSKRLFK....LAAQATRY.GE
Spy QSI....MDLYHGLENF............DPSNREGHAARIYFNTLFG...N.......
Eco PA.....RRSVEQLRGI.....EGSRVRA....TY.ALLAKQYG....VTWNGRRY...
Pat EHLQ...ALLDRYQKGL.....TDCRTSNDVLVQEAMMTKALYR....LAANAVSY.GD
Afu ESLLKAKKEIDACLNELDGVEAEMIDKVRERLLGIEGKASKHYWDAISLVIPEEYRFNGR
Tma ..A....DSLTRYKKKA.....EEASNVSELMGIEGNAREEYYSMIDSLVSDE..R...
Aae ..K....ISADTYLNKV.....KETNSIPELMSVEAEFRKLCYKKLEE...VT..G...
Lin SYL....ATIRSGLKNI.....ESADSPSQLLGIEGSSARAYFSGLPALLKNSDPF...

α8 α9
Pae TT   210   220   230   240   TT   250   260

Pae FVR..AKRGSGGDPANRFLDHGNYLAYGLAATATWVLGIPHGLAVLHGK.TRRGGLVFDV
Spy .....DFSRDLEHPINAGLDYGYTLLLSMFAREVVVSGCMTQFGLKHANQFNQFNFASDI
Eco ..D..PKDWEKGDTINQCISAATSCLYGVTEAAILAAGYAPAIGFVHT..GKPLSFVYDI
Pat FTR..AKRGGGTDLANRFLDHGNYLAYGLAAVSTWVLGLPHGLAVLHGK.TRRGGLVFDV
Afu RGIEIGSPRYAKDIVNAMLNYGYSILLAECVKAVELAGLDPYAGFLHVDVSGRSSLAIDL
Tma FRIEKRTRRPPKNFANTLISFGNSLLYTTVLSLIYQTHLDPRIGYLHETNFRRFSLNLDI
Aae WELEKRTKRPPQNPLNALISFGNSLTYAKVLGEIYKTQLNPTVSYLHEPSTKRFSLSLDV
Lin LVPNGRSKRPPKDPFNATLSFLYSLLYKSVRQAIIAVGLDPSFGFYHTPRSSAEPLVLDL

α10 α11 α12
Pae ℓ   270   280   290   300   310   320

Pae ADLIKDSLILPQAFLSAMR..GDEEQDFRQA...CL.DNLSRAQALDFMIDTLKDVAQRS
Spy MEPFRPLVDKIVYENRNQPFPKIKRELFTLFSD..TFSYNGKEMYLTNIISD.......
Eco ADIIKFDTVVPKAFEIARRNPGEPDREVRLA...CR.DIFRSSKTLAKLIPLIEDVLAAG
Pat ADLIKDALVLPQAFIAAME..GEDEQEFRQR...CL.TAFQQSEALDVMIGSLQDVASKL
Afu MENFRQQVVDRVVLRLIS.YRQIKPEDCEKRNMVCQLSDNARRLLLASLLERLDSKTQY.
Tma AELFKPAVVDRLFLNLVN.TRQINEKHFDEISEGLMLNDEGKSLFVKNYEQALRETVFH.
Aae AEVFKPIFVDNLIIRLIQ.ENKIDKTHFSTELNMTFLNEIGRKVFLKAFNELLETTIFY.
Lin MELFRVSLCDMTLIGSIN.RKSWIDEDFEITKNKVWLSESGRKKATQLYETRLDDTWKH.

Fig. 3. Multiple sequence alignment of Cas1 orthologs with LinCas1 to identify the metal-interacting residues. The MSA was performed using the program Clustal Omega. The LinCas1 (Lin; Q72TS5) sequence of CRISPR-Cas I-B are compared with the known Cas1 sequence of the *Pseudomonas aeruginosa* (Pae; Q02ML7), *Streptococcus pyogenes* (Spy; J7M1H5), *Escherichia coli* (Eco; Q46896), *Archaeoglobus fulgidus* (Afu; O28401), *Pectobacterium atrosepticum* (Pat; Q6D0 × 0), *Thermotoga maritima* (Tma; Q9 × 2B7), and *Aquifex aeolicus* (Aae; O66692). Secondary structure elements are indicated based on the known crystal structure of PaeCas1. Three conserved metal-ion binding residues (Glu108, His176 and Glu191) of LinCas1 are highlighted with the blue sphere. Other conserved residues such as Asn145 and Asp188 present in the vicinity of the metal-ion binding site are highlighted with the green triangle. Only the partial MSA has been shown for the clarity of the figure. (For interpretation of the references to color in this figure legend, the reader is referred to the web version of this article.)

binding pocket of LinCas1 are also found to be conserved among Cas1 orthologs (Fig. 3). The chemical niche of the LinCas1 metal-ion binding site is similar to that of the Cas1 orthologs, which ascertains a familiar role in diverse CRISPR-Cas subfamilies (Wiedenheft et al., 2009; Yosef et al., 2012; Kim et al., 2013; Wilkinson et al., 2016).

The closest structural homolog of LinCas1 in the Protein Data Bank (PDB) shows Cas1 from *T. maritima* (TmaCas1) with an RMSD (root mean square deviation) of 0.6 Å (Table 2). The tertiary structure of LinCas1 monomer, modelled using TmaCas1 as the template, revealed the presence of two structurally distinct domains composed of α1-β1-β2 (NTD) and α2-α3-α4-α5-η1-α6-α7-β3-β4-α8-β5-β6-α9 (CTD) secondary folds connected by a linker (Fig. 4A). The modelled CTD [amino acid (aa) 32–284] of LinCas1 protomer consists of eight α-helices (grey; α2–α9), one 3₁₀ helix (grey) and four β-strands (orange; β3–β6) (Fig. 4A). Although the overall structure of the CTD in LinCas1 from various organisms is similar, the number of α-helices and β-strands slightly varies. For instance, the CTD (aa 95–305; α2–α8) of EcoCas1(Babu et al., 2011) and PaeCas1 (aa 113–324; α3–α10)(Wiedenheft et al., 2009) is an all-helical structure while in the case of LinCas1 four additional β-strands (orange) are present (Fig. 4A and B). Such an additional four β-strands in CTD have also been reported in AfuCas1(Kim et al., 2013)

and AaeCas1 (PDB ID: 2YZS). However, these structural variations do not significantly affect the enzymatic activity of Cas1 as they are located far apart from the putative nucleolytic core (Kim et al., 2013). The metal-ion binding pocket in LinCas1 is located between α5 and α7 helices of the CTD (Fig. 4A) and agrees with the reported structure of AfuCas1 (Kim et al., 2013).

Incredibly, the NTD (cyan and blue) of LinCas1 is much shorter than that of other Cas1 orthologs (Fig. 4A and B) (Wiedenheft et al., 2009; Babu et al., 2011; Kim et al., 2013). The NTD of LinCas1 comprises of two β-strands (blue) and one α-helix (cyan), whereas, EcoCas1 possesses one α-helix (pink), two 3₁₀ helices and eight β-strands (magenta) (Fig. 4A and B) (Babu et al., 2011). The NTD of PaeCas1 is composed of ten β-strands and two α-helices whereas that of AfuCas1 contains one α-helix and eight short β-strands (Wiedenheft et al., 2009; Kim et al., 2013). Variations in LinCas1 secondary structure prompted us to model the dimeric form of LinCas1 as NTD of Cas1 has been described to play a significant role in the formation of homo-dimer in an asymmetric fashion through hydrogen bond and salt bridges (Wiedenheft et al., 2009). In general, the homo-dimer of the Cas1 protein from all organisms attains a butterfly-like shape (Fig. 4C and D). Modelling of homo-dimer of LinCas1 using the available crystal structures shows a
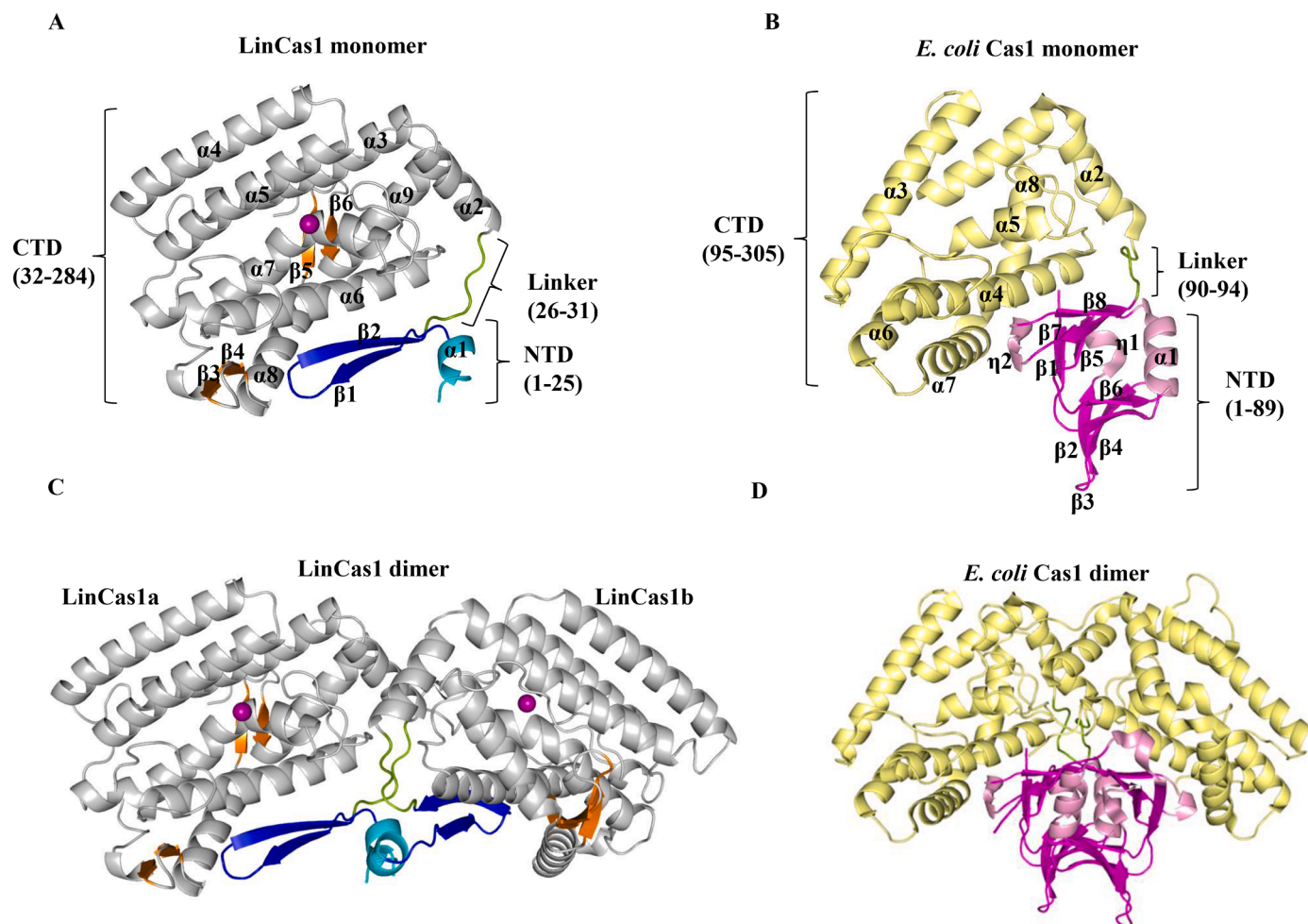
Fig. 4. Structural comparison of modelled LinCas1. (A) The modelled tertiary structure of LinCas1 is shown with its N- and C-terminal domains (NTD and CTD) connected by a linker shown in green. The secondary structure of α-helices/β-strand in the NTD and CTD are shown in cyan/blue and grey/orange, respectively. The metal-ion interacting site is represented with a purple sphere. (B) The tertiary structure of Cas1 monomer of *E. coli* for comparison with LinCas1. The NTD is shown in pink (α-helix) and magenta (β-strand) color. The secondary structure of the CTD and linker region is shown in yellow and green colors, respectively. (C) The modelled homo-dimer of LinCas1 is shown as a cartoon. The model suggests that it is asymmetric in nature, with its metal-ion binding pocket of each subunit demarcated as LinCas1a and LinCas1b facing in the opposite direction. (D) The tertiary structure of Cas1 homo-dimer of *E. coli* is shown for comparison with LinCas1. The figure indicates that LinCas1 has a shorter NTD compared to EcoCas1. (For interpretation of the references to color in this figure legend, the reader is referred to the web version of this article.).

similar shape.

Also, a selective Cas1 evolutionary and comparative analysis with LinCas1 binding regions (metal-ion) was determined. The molecular phylogeny of LinCas1, along with other Cas1 orthologs, reveals LinCas1 closeness to thermophilic organisms (Fig. S3A). It is observed that at the secondary structure level, due to extra β-strands (CTD), LinCas1 is relatively closer to AfuCas1 than EcoCas1 and PaeCas1. Also, the recently published molecular phylogeny of another core protein, Lin-Cas2 of CRISPR-Cas in *Leptospira*, shows its lineage closer to Cas2 of *S. solfataricus* than *B. halodurans*, which is another thermophilic archaeon (Dixit et al., 2016). Under the MSA of Cas1 orthologs (Fig. 3), the metal-ion coordinating residues typically found among nucleases are conserved at the tertiary structure of the modelled LinCas1. More precisely, the LinCas1 residues (Glu108, His176 and Glu191) and PaeCas1 residues (Glu190, His254 and Asp268) coordinate the divalent-metal (most probably Mn^{2+}) ion. Comparative analysis of metal-ion binding pocket at the tertiary level of LinCas1 (cyan) with PaeCas1 (pale yellow) shows a preference for Mn^{2+} than Mg^{2+} (Fig. S3B).

2.3. Mutation of residues involved in coordinating metal-ion in LinCas1 compromises its activity

Based on multiple sequence alignment of Cas1 proteins, site-directed mutagenesis of the predicted metal-ion binding residues (Glu108, His176, and Glu191) of LinCas1 was performed. The mutant LinCas1 variants (LinCas1E108A, LinCas1H176A, and LinCas1E191A) were overexpressed and purified with a similar yield (Fig. S1C and D). The nuclease activity of mutants LinCas1 (E108A), (H176A), and (E191A) was on expected lines, as there occurs dramatic loss in the endonuclease activity on circular ss-DNA (Fig. 5). This leads us to conclude that Lin-Cas1 possesses metal-ion dependent DNase activity as previously reported in other Cas1 orthologs (Wiedenheft et al., 2009; Babu et al., 2011; He et al., 2018).

2.4. In vitro characterization of Cas1-Cas2 protein interaction

Nuclease assays of core LinCas proteins (LinCas1 and LinCas2) in this study and other reported studies by Dixit et al. (2016), reveals that these core LinCas proteins possess metal-dependent DNase activity. In *E. coli* (CRISPR type I-E) and *E. faecalis* (CRISPR type II-A), the Cas1-Cas2
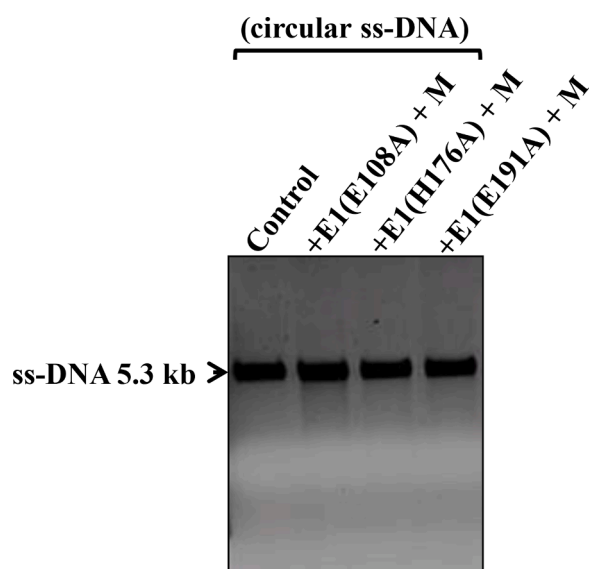
Fig. 5. Mutant LinCas1 nuclease activity on ss-DNA. E1 represents LinCas1, and M denotes Mn^{2+}. All the reactions were carried out for 1 h at 37 °C. Substitution of metal interacting residues (Glu108, His176, and Glu191) in LinCas1 with Ala leads to loss of nuclease activity on circular ss-DNA (ϕx174 genome; 5.3 kb).

complex has been reported to form an asymmetric heterohexameric complex consisting of two Cas1 dimers that sandwich one Cas2 dimer (Nuñez et al., 2015; Xiao et al., 2017). It was thus interesting to address whether the nuclease activity is altered when core LinCas proteins are mixed. In addition, the NTD of LinCas1 responsible for interacting with LinCas2 is shorter than its Cas1 orthologs. Thus, nuclease assay with a mixture of LinCas proteins may address the impact of short NTD of LinCas1 over LinCas2. Based on this, a complex of LinCas1-Cas2 was generated under *in vitro* condition by incubating pure LinCas1 and LinCas2 in a 2:1 molar ratio, as suggested elsewhere (Nuñez et al., 2015). The activity of the LinCas1-Cas2 mixture on the DNA substrate (linearized ds-DNA pTZ57R/T) shows a reduction in DNA cleavage and a shift in the mobility of DNA during agarose gel electrophoresis (Fig. 6A). However, the pure LinCas1 at an equivalent molar concentration shows intense nuclease activity on ds-DNA (Fig. 6A).

Due to the constraints in purifying LinCas1 at higher concentrations (Fig. S1), a lower amount of LinCas2 was incubated (3 μM) with LinCas1 (6 μM) to generate the mixture (2:1) for nuclease activity on ds-DNA (Fig. 6A). Nuclease activity was not detected at a lower concentration of pure LinCas2 (3 μM); however, LinCas2 at higher concentration (20 μM) exhibits nuclease activity (Fig. 6A), as reported previously (Dixit et al., 2016).

Next, in the LinCas1-Cas2 mixture, we addressed whether mutating the residues (involved in metal-ion binding) of LinCas1 will affect its affinity for DNA. Therefore, LinCas2 was mixed with one of the mutants LinCas1(E108A). The nuclease assay revealed a loss of the cleavage activity in LinCas1(E108A) and LinCas2 mixture on circular ds-DNA similar to that of LinCas1-Cas2 mixture (Fig. 6B). However, LinCas1 (E108A) does show a change in the conformation of circular ds-DNA from supercoiled to relaxed form, possibly due to a moderate nick (Fig. 6B). Nevertheless, the alteration in the activity of the LinCas1 (E108A)-Cas2 mixture for ds-DNA was in agreement with LinCas1-Cas2 mixture, where LinCas2 promotes the binding affinity of LinCas1 (E108A) for ds-DNA (Fig. 6C). Such findings agree with the recorded information about the EcoCas2 dimer. In *E. coli*, the EcoCas2 dimer act as an adaptor protein, bring two EcoCas1 dimers together to stabilize and scale the length of the protospacer DNA (Wang et al., 2015). The Cas1-Cas2 complex selects the protospacer based on the flanking protospacer adjacent motif (PAM) sequence and processes it into appropriate sizes while also cleaving off the PAM sequence, and integrates

them between the first CRISPR repeat and leader sequence upstream of the CRISPR array (Barrangou et al., 2007; Yosef et al., 2012; Wei et al., 2015). Recently, through a computational approach, a weakly conserved PAM sequence (5′-TAC-3′) for the *Leptospira* CRISPR-Cas I-B has been identified (Xiao et al., 2019). In the LinCas1 and LinCas2 interaction study, the substrate (ds-DNA and linearized pTZ57R/T used has about 60 such PAM motifs. These PAM motifs (5′-TAC-3′) may direct the LinCas1-Cas2 mixture to recognise protospacers in the substrate pTZ57R/T for the adaptation process. Nevertheless, further *in vivo* and *in vitro* studies are required to confirm this hypothesis and understand the adaptation process of the CRISPR-Cas system in *Leptospira*.

Additionally, the interaction between the core LinCas proteins (LinCas1 and LinCas2) was addressed by performing an enzyme-linked immunosorbent assay (ELISA) using antibodies generated against Lin-Cas2 (anti-LinCas2). Microtiter plate was coated with LinCas1 (100 ng) or bovine serum albumin and was overlaid with LinCas2 at an increasing concentration (5 ng–12.8 μg). At 450 nm of absorbance, specific interaction was demonstrated between LinCas2 and LinCas1 that could achieve a saturation point (Fig. 6D). The ELISA data supports our previous finding that LinCas1 and LinCas2 mixture interact to form a functionally regulated Cas1-Cas2 complex. The dissociation constant (K_d) of the LinCas2 to LinCas1 interaction through ELISA was 12.86 ± 1.73 nM with a stoichiometry of 0.88. Moreover, in support of ELISA, an immunoblot was performed to demonstrate recombinant LinCas2 existence in monomer and homo-dimer form on SDS-PAGE (Fig. 6E). Monomers and dimer forms of native LinCas2 could be detected through immunoblot in the lysate of *L. interrogans* serovar Copenhageni (Fig. 6F). Faint bands in immunoblot obtained from the lysate (5×10^9 cells in 50 ml) of spirochete suggest that the expression level of cas2 in *Leptospira* is minimal (Fig. 6F).

The activity of LinCas1-Cas2 mixture was also investigated on the ss-DNA oligonucleotide (37 mer) sequence with no PAM motif (5′-TAC-3′). The LinCas1-Cas2 did not show oligonucleotide (37 mer) cleavage on denaturing PAGE (Fig. S4A). However, on native PAGE, a shift in the mobility of a small proportion of oligonucleotides was detected when incubated with pure LinCas1 or LinCas1-Cas2 (Fig. S4B). The shift in the mobility of the oligonucleotide in the presence of pure LinCas1 or LinCas1-Cas2 mixture appears to be similar, which suggests that LinCas1 interacts with the ss-DNA oligo (Fig. S4B).

This study witnessed an alteration in LinCas1 nuclease activity similar to *E. coli* and *E. faecalis* Cas1-Cas2 (Nuñez et al., 2015; Xiao et al., 2017). In addition to this, several other attempts were made to understand the association between LinCas1 and LinCas2. Owing to the high isoelectric point (pI >9.5) of LinCas1 and LinCas2, the protein complexes on native PAGE carried a strong positive charge and thus deterred its migration on the gel. Reversing the direction of the electrode assembly in the native PAGE also failed to resolve the complex. The size exclusion chromatography could not be accomplished to study the interaction between LinCas1 and LinCas2 due to the low yield and concentration of purified LinCas1.

3. Discussion

Biochemical analysis of the LinCas1 reveals that it possesses endonuclease activity in the presence of specific divalent-metal, particularly Mn^{2+}, which stands in agreement with the reported preference of divalent metal-ion for ds-DNase activity in the Cas1 orthologs of *Pseudomonas aeruginosa* (PaeCas1) and *Riemerella anatipestifer* (RanCas1) (Wiedenheft et al., 2009; He et al., 2018). In contrast, the DNase activity in AfuCas1 of *Archaeoglobus fulgidus* was observed in the presence of Ca^{2+} and Ni^{2+} metal-ion (Kim et al., 2013). Thus, the specificity of divalent-metal for nuclease activity varies among various characterized Cas1 proteins, which probably depends on the negatively charged residues interacting with the divalent-metal-ion. The LinCas1 (Glu108 and Glu191) and PaeCas1 (Glu190 and Asp268) attract positively charged metal-ions such as Mn^{2+} and Mg^{2+}. However, the presence of histidine
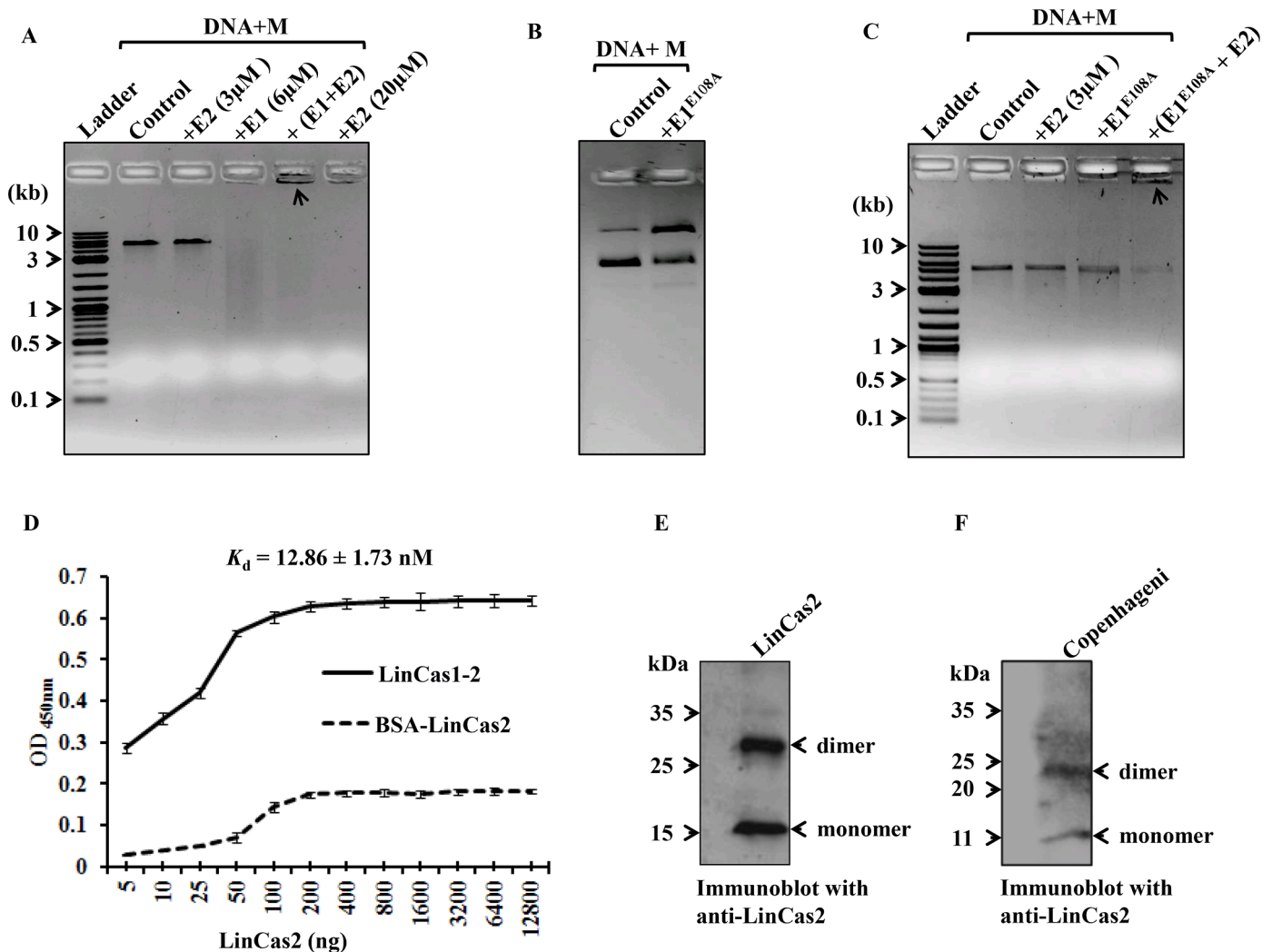
Fig. 6. LinCas1-Cas2 mixture nuclease activity under *in vitro* condition on linear ds-DNA. (A) Activity of LinCas1-Cas2 mixture on linear ds-DNA. The nuclease activity of LinCas1-Cas2 (E1-E2) mixture on the substrate (linearized ds-DNA pTZ57R/T; 2.9 kbp) shows a reduction in DNA cleavage and a shift in the mobility of DNA (arrow marked) in the agarose gel electrophoresis. However, the equimolar concentration of pure LinCas1 (E1; 6 μM) shows intense nuclease activity on DNA. This indicates a change in the biochemical activity of LinCas1-Cas2 mixture than that of the equal molar concentration of pure LinCas1 (E1; 6 μM) or LinCas2 (E2; 3 μM). (B) Substitution of metal-ion binding residue in LinCas1 (E1) leads to a loss in nuclease activity on circular ds-DNA. Nuclease activity of mutant E1 (E1^{E108A}) on circular ds-DNA shows no cleavage in the presence of divalent-metal. However, due to the moderate nick, intensity of the relaxed form of plasmid was increased. Control lane show multiple bands corresponding to different conformations of plasmid DNA. (C) Nuclease activity in a mixture of mutant LinCas1 (E1^{E108A}) and LinCas2 (E2) or its pure form is dramatically reduced on linear ds-DNA. The mixture (E1^{E108A}+E2) shows a reduction in DNA (pTZ57R/T) cleavage activity and shift in mobility of DNA (arrow marked) in the agarose gel electrophoresis. (D) Immunoassay of LinCas1 and LinCas2 interaction under *in vitro* condition. LinCas1-Cas2 interaction study was done using enzyme-linked immunosorbent assay (ELISA). Microtiter plates were coated with LinCas1 (100 ng) or as a negative control with bovine serum albumin (BSA). Thereafter, LinCas2 at an increasing concentration was overlaid on it as an interacting partner. LinCas2 interacted with LinCas1 and reached a point of saturation when probed with anti-LinCas2 (1:1000) and HRPO-conjugated secondary antibodies (1:5000) with TMB (Trimethylbenzidine) as a substrate. The absorbance was measured at 450 nm after terminating the reaction using 1M H$_2$SO$_4$. (E) An immunoblot to detect LinCas2 in monomer (~13 kDa) and homo-dimer (~27 kDa) form using anti-LinCas2. (F) Immunoblot of *L. interrogans* serovar Copenhageni lysate with anti-LinCas2. Two bands of the native LinCas2 at monomer (~11 kDa) and dimer (~22 kDa) size were detected.

residue in LinCas1 (His176) and PaeCas1 (His254) along with negatively charged residues shifts its preference towards Mn^{2+}, as discussed elsewhere (Khrustaleva, 2014). Furthermore, the preference for monovalent-ions for LinCas1 nuclease activity also agrees with the earlier reported activity in PaeCas1 (Wiedenheft et al., 2009). The nuclease activity of LinCas1 on viral DNA substrates is consistent with the nuclease activity reported in PaeCas1 (Wiedenheft et al., 2009). However, LinCas1 inability to cleave short oligos is contentious to the activity reported in EcoCas1, where it cleaves short ss-DNAs as well (Babu et al., 2011). The cleavage of ss-DNA is essential in the processing of the protospacer bound by the Cas1-Cas2 complex prior to its integration in the CRISPR loci (Yosef et al., 2012; Nuñez et al., 2014, 2015;

Levy et al., 2015; Wang et al., 2015; Xiao et al., 2017; He et al., 2018; Kieper et al., 2018; Rollie et al., 2018). The LinCas1 disability to act on short ss-DNAs, perhaps can be compensated by the activity of the LinCas4 in *L. interrogans*, which has been recently reported to cleave short oligos under *in vitro* condition (Dixit et al., 2021). In numerous prokaryotes harboring different CRISPR-Cas subtypes, Cas4 orthologs has been established to be essential for spacer acquisition with high fidelity in association with Cas1 and Cas2 including *Bacillus halodurans* (type I-C) (Lee et al., 2018), *Sulfolobus islandicus* (type I-A) (Liu et al., 2017), *Geobacter sulfurreducens* (type I-U) (Almendros et al., 2019), *Synechocystis* sp. 6803 (Kieper et al., 2018), and *Haloarcula hispanica* (type I-B) (Li et al., 2014).

The substitution of Glu108, His176, and Glu191 residues with Ala in LinCas1 showed a drastic reduction in its DNase activity, similar to the loss of the DNase activity reported in PaeCas1 (D268A), EcoCas1 (H208A and D221A), and RanCas1 (E149A, H206A, and E221A), respectively (Wiedenheft et al., 2009; Babu et al., 2011; He et al., 2018). The metal-ion interacting residues (Glu108, His176, and Glu191) in the LinCas1 correspond to the similar residues in different CRISPR-Cas subtypes, including I-A (*S. solfataricus*), I-F (*P. atrosepticum*), and I-E (*E. coli*) (Yosef et al., 2012; Wilkinson et al., 2016; Rollie et al., 2018). The metal-ion interacting residues in these Cas1 orthologs are illustrated to be essential for integrase activity. Mutagenesis studies suggest that the interacting metal residues of the LinCas1 may conceivably be crucial for the CRISPR acquisition in the *L. interrogans*.

The existence of a shorter NTD in LinCas1 compared to its orthologs did not hinder its interaction with LinCas2, which was confirmed through ELISA demonstrating a high affinity of LinCas2 to LinCas1 interaction ($K_d = 12.86 \pm 1.73$ nM). In contrast, the Cas1 affinity of *E. coli* (Nuñez et al., 2014) and *S. pyogenes* (Ka et al., 2018) to its cognate Cas2 by isothermal titration calorimetry was weaker ($K_d = \sim 290$ and 240 nM, respectively). Also, the nuclease assay of the *in vitro* generated LinCas1-Cas2 complex demonstrates alteration in the nuclease activity of the pure-LinCas1. Notably, a previous study reported that the protospacer binding to the EcoCas1-Cas2 complex triggers large structural rearrangements within the core Cas protein (Wang et al., 2015). Thus we speculate that LinCas1, upon forming a complex with LinCas2, undergoes structural rearrangements leading to a change in the nuclease activity.

Interestingly, bacterial cells (*E. coli*) grew normally after LinCas1 overexpression, which suggests that the genomic DNA of *E. coli* was not much influenced by the LinCas1 nuclease activity during the 20 min of generation time. Based on the *in vitro* nuclease assays of the LinCas1, it is possible that the host genomic DNA remains intact due to the lack of required optimum concentrations of divalent and monovalent ions within the *E. coli*. Similarly, on overexpressing LinCas1 and LinCas2 together in *E. coli*, there occurred no deleterious effect on the host genomic DNA.

Plasmids such as pMaOri (around 5 kbp) and pMaOri.dCas9 (around 10 kbp) in *L. interrogans* has been reported to be maintained for several passages (Fernandes et al., 2021). Based on the nuclease activity of LinCas1 on circular ds-DNA (pTZ5R/T plasmid), which possesses numerous ($n = 60$) PAM motifs (5'-TAC-3), we believe that under *in vitro* conditions, LinCas1 may also be able to cleave pMaOri and pMaOri.dCas9 plasmids by recognizing its PAM motifs (5'-TAC-3). On the contrary, under *in vivo* conditions, the expression level of the native Cas1 may be minimal similar to that of LinCas2. Moreover, the influence of different divalent and monovalent ions within the *Leptospira* may modulate its nuclease activity on plasmids. The other plausible reason for the stability of the exotic plasmids (pMaOri and pMaOri.dCas9) in *Leptospira* spp. could be due to the occurrence of only primed adaptation as has been reported in type I-B system of *Haloarcula hispanica* (Li et al., 2014). In primed adaptation, aside from the adaptation proteins (Cas1, Cas2, and Cas4), a pre-existing spacer is a prerequisite to initiate CRISPR adaptation (Li et al., 2014).

In *L. interrogans* serovar Copenhageni, the adaptation modules of I-B (cas1, cas2, and cas4) involved in adaptation have been reported to be actively transcribed under *in vitro* growth conditions (Dixit et al., 2016). In this study, native LinCas2 protein has been shown to be expressed in *L. interrogans* which is contrary to the previous finding where quantitative proteome analysis of *L. interrogans* did not reveal cas2 gene expression (Malmström et al., 2009). This discrepancy can be reasonably explained due to the low differential expression level of the cas2 gene.

4. Conclusion

The results of this study demonstrate that LinCas1 is biochemically active like LinCas2 and LinCas4 of the CRISPR-Cas I-B in *Leptospira*. The

data presented here ascertain that the LinCas1 has versatile nuclease activity and can interact with LinCas2 despite its short NTD. The diverse DNA substrates that can be cleaved by LinCas1 enable us to determine the substrate types that can be used as a possible source of protospacers for CRISPR adaptation in *Leptospira*. The DNase activity for LinCas1 is consistent with a role for this protein in the recognition/cleavage of foreign DNA and integration as a new spacer into the CRISPR array (Nuñez et al., 2015; Rollie et al., 2018). Further detailed analysis of the role of LinCas1 in the CRISPR adaptation mechanism within *Leptospira* requires using a natural experimental model as established in *E. coli* CRISPR spacer integration.

5. Materials and methods

5.1. Bacterial strains

The bacterial strain of *L. interrogans* serovar Copenhageni Fiocruz L1-130 was procured from the Indian Council of Medical Research (ICMR), Regional Medical Research Centre, Port Blair, Andaman and Nicobar Island, India. High-passaged *Leptospira* were cultured in EMJH (Ellinghausen-McCullough-Johnson-Harris, Difco) medium at 29 °C and sub-cultured at 7-days intervals to isolate genomic DNA. Bacterial strains of *E. coli* DH5α and BL21 (DE3) were grown at 37 °C in LB (Luria Bertani) medium or agar for cloning, transformation, and expression.

5.2. Recombinant DNA techniques and nucleic acid isolation

Genomic DNA of *L. interrogans* serovar Copenhageni was isolated from a 7-day old 10 ml culture using a bacterial genomic DNA purification kit (Qiagen), as per the manufacturer's instruction. Plasmids were isolated from 5 mL of an overnight culture of *E. coli* using a plasmid purification kit from New England Biolabs (NEB). Standard procedures were used for the generation of the recombinant plasmid. The QIAquick gel extraction kit (Qiagen) was used to isolate DNA fragments from agarose gels. Substrate ss-DNA (M13mp18, φx174) and all enzymes used for genetic engineering were sourced through NEB or Fermentas. The confirmed clones were outsourced to Eurofins Genomics India Pvt. Ltd, Bengaluru for DNA sequencing before purification and characterization of proteins.

5.3. Nuclease activity assays

Nuclease activity in LinCas1 was investigated on various DNA substrates, as described elsewhere (Beloglazova et al., 2015). The different nucleic acid substrates (1.0 μg each) used for evaluating the nuclease activity of LinCas1 were circular double-stranded (ds) DNA plasmid (pTZ57R/T), linear ss-DNA (M13mp18), circular ss-DNA (φx174 genome), and short oligos of 28 & 37 mer sequence with no PAM (5'-TAC-3') motif (Xcelris Genomic India). These substrates (1.0 μg) were incubated with the purified rLinCas1 (active) or its heat-inactivated (100 °C for 10 min) form (6 μM each) in a 25 μl reaction buffer (25 mM HEPES pH 7.0, 100 mM KCl, and 2.5 mM MnSO4) at 37 °C for 1 h unless stated. To chelate the metals in the nuclease reaction EDTA (10 mM) was used at the specified reaction condition. Preference for divalent-metal for nuclease activity was determined by substituting Mn^{2+} with various other metal-ion like Mg^{2+}, Ca^{2+}, and Ni^{2+} ions. The optimal pH was determined by substituting the buffer with either 25 mM sodium citrate (pH 3.0 to 5.0), MES (pH 6.0), HEPES (pH 7.0), Tris-HCl (pH 8.0), or CAPS (pH 9.0 to 11.0). The effect of monovalent-ions on LinCas1 nuclease activity was studied using NaCl, KCl, and NH4Cl, at varying concentrations (50–150 mM). The time-bound nuclease assay was performed to determine the duration required to cleave the substrate completely. All the above resulting reaction products were separated on 0.8% (w/v) agarose gel electrophoresis except the short oligo (ss-DNA) reaction products which were separated on an 18% (w/v) 8 M denaturing Urea PAGE, stained with ethidium bromide and visualized in

gel documentation instrument (Biorad, Hercules, CA, USA).

5.4. Site-directed mutagenesis

The potential metal-ion binding amino acids in the LinCas1 were mutated using the Q5 site-directed mutagenesis kit (NEB) and pET28a-LinCas1 plasmid construct. Primers were designed (Table 1) using the NEBaseChanger tool program to mutate residues Glu108/191 (codon GAA) to Ala (GCA) in LinCas1. Similarly, His176 (CAC) was substituted with Ala (GCC). All the derived mutants were confirmed by sequencing before purification of the proteins using Ni-NTA chromatography.

5.5. Biochemical and immunoassay for Cas1-Cas2 interaction

Generation of LinCas1-Cas2 complex under *in vitro* condition was done by incubating LinCas1 (10 μM) and LinCas2 (5 μM) at 4 °C in 2:1 molar ratio for 1 h. A nuclease reaction was set up at 37 °C for 1 h using the LinCas1-Cas2 complex (6:3 μM) and 1 μg of linear ds-DNA (pTZ57R/T) or ss-DNA oligonucleotide (37 mer) as the substrate in a nuclease buffer (25 mM Tris-Cl, 100 mM KCl and 10 mM Mg^{2+}). A similar nuclease reaction was set up containing an equal molar concentration of pure LinCas1 (6 μM) or LinCas2 (3 μM) independently along with linear ds-DNA. The resulting reaction products were resolved on 0.8% agarose gel, stained with ethidium bromide, and visualized in a gel documentation instrument.

Antibodies against recombinant LinCas2 proteins were generated in rabbits by outsourcing the purified proteins to Abgenex, Bhubaneswar, India. Microtiter plates were coated with 50 μl of recombinant LinCas1 proteins or bovine serum albumin (BSA) as control (100 ng/well) overnight at 4 °C. Thereafter, the unbound LinCas1 protein was discarded from the wells, and each well was blocked with 3% bovine serum albumin (BSA) solution for 2 h at 37 °C and then was overlaid by LinCas2 at an increasing concentration ranging from 5 ng to 12.8 μg per well for 2 h at room temperature. After three washes of each well with 0.05% phosphate buffer saline-Tween 20 (PBS-T) buffer, anti-LinCas2 at 1:1000 dilutions was used to find the interaction between LinCas2 and LinCas1 and detected using HRP-conjugated anti-rabbit secondary antibodies (1:5000) with TMB (Trimethylbenzidine, Thermo scientific) as substrate. The absorbance was measured at 450 nm after terminating the reaction using 1 M H_2SO_4 as per the manufacturer's instruction. The results are indicative of the average of two independent experiments. The dissociation constant and stoichiometry of LinCas2 to LinCas1 interaction was calculated by nonlinear curve fitting using the Hill function in OriginPro 8.5 software. For immunoblot assay, purified rLinCas2 (5 μg/lane) and whole-cell lysate of *L. interrogans* serovar Copenhageni (~5 × 10^9 spirochetes/lane) were resolved on 12% SDS-PAGE, transferred to a nitrocellulose membrane, and probed with anti-LinCas2 rabbit immune sera (1:1000 and 1:500, respectively). The immunoblot was developed by adding HRP-conjugated secondary antibodies (1:5000) and enhanced chemiluminescence as previously described (Kumar et al., 2011).

5.6. Multiple sequence alignment of Cas1 orthologs and structure predictions

In a search for the conserved metal-ion coordinating residues, a multiple sequence alignment (MSA) of Cas1 protein sequences from *L. interrogans, Streptococcus pyogenes, Archeoglobus fulgidus, Aquifex aeolicus, Thermotoga maritima, Pseudomonas aeruginosa* and *Pectobacterium atrosepticum* was performed using the program Clustal Omega with a default set of parameters (Sievers and Higgins, 2014). The aligned sequences were further rendered using the online web server ESPript (Easy Sequencing in PostScript) (Gouet et al., 2003). The amino acid sequences of all the Cas1 proteins from various organisms were downloaded from the UniProtKB database (https://www.uniprot.org/). Structural homologs of LinCas1 were obtained using the Dali server

Table 1
Primer sequences used in this work.

5′ to 3′ Sequence	Purpose
CTAGCTAGCATGATTAAATTTTTAGTTTCCGAAGAG	Forward primer LinCas1 (*LIC10942*) *Nhe*I
CCGCTCGAGTTATCTTAACCTCGCTTGTGCA	Reverse primer LinCas1 (*LIC10942*) *Xho*I
ATTAGGGATCGcAGGTTCGTCGG	Forward primer for the LinCas1(E108A) mutation
AATTGACTTGGGGAATCCG	Reverse primer for the LinCas1(E108A) mutation
CGGTTTTTATgcCACTCCAAGATCTTC	Forward primer for the LinCas1(H176A) mutation
AAACTTGGATCGAGACCAAC	Reverse primer for the LinCas1(H176A) mutation
AGATTTAATGgcACTTTTCCGTGTAAG	Forward primer for the LinCas1(E191A) mutation
AAAACAAGAGGTTCGGCG	Reverse primer for the LinCas1(E191A) mutation
CTAGCTAGCTTGGAAGGAGGTCCTTTGG	28 mer oligo
CTAGGATCCCATGATTAAATTTTTAGTTTCCGAAGAG	37 mer oligo

Table 2
Tertiary structure homologues of LinCas1 using Dali search program.

Protein	PDB ID	Organism	RMSD (Å)	Z-score*
Cas1	4XTK	*Thermotoga maritime*	0.6	37.7
Uncharacterized	2YZS	*Aquifex aeolicus*	1.6	29.4
Cas1	5DQU	*Escherichia coli*	2.2	18.3
Cas1	4N06	*Archaeoglobus fulgidus*	2.5	26.5
Cas1	3GOD	*Pseudomonas aeruginosa*	2.7	19.2
Cas1	5FCL	*Pectobacterium atrosepticum*	2.8	19.3
Cas1	4ZKJ	*Streptococcus pyogenes*	3.7	16.1

*Higher Z-scores correspond to structures which agree more closely in architectural detail.

(Holm and Rosenstrom, 2010).

Declaration of Competing Interest

The authors declare that they have no known competing financial interests or personal relationships that could have appeared to influence the work reported in this paper.

There are no conflicts to declare

Supplementary materials

Supplementary material associated with this article can be found, in the online version, at doi:10.1016/j.crmicr.2021.100059.

References

Almendros, C., Nobrega, F.L., McKenzie, R.E., 2019. Brouns SJJ. Cas4–Cas1 fusions drive efficient PAM selection and control CRISPR adaptation. Nucleic Acids Res. 47 (10), 5223–5230.

Arbas, S.M., Narayanasamy, S., Herold, M., Lebrun, L.A., Hoopmann, M.R., Li, S., Lam, T. J., Kunath, B.J., Hicks, N.D., Liu, C.M., 2021. Roles of bacteriophages, plasmids and CRISPR immunity in microbial community dynamics revealed using time-series integrated meta-omics. Nat. Microbiol. 6 (1), 123–135.

Babu, M., Beloglazova, N., Flick, R., Graham, C., Skarina, T., Nocek, B., Gagarinova, A., Pogoutse, O., Brown, G., Binkowski, A., Phanse, S., Joachimiak, A., Koonin, E.V., Savchenko, A., Emili, A., Greenblatt, J., Edwards, A.M., Yakunin, A.F., 2011. A dual function of the CRISPR-Cas system in bacterial antivirus immunity and DNA repair. Mol. Microbiol. 79 (2), 484–502.

Barrangou, R., Fremaux, C., Deveau, H., Richards, M., Boyaval, P., Moineau, S., Romero, D.A., Horvath, P., 2007. CRISPR provides acquired resistance against viruses in prokaryotes. Science 315 (5819), 1709–1712.

Beloglazova, N., Lemak, S., Flick, R., Yakunin, A.F., 2015. Analysis of nuclease activity of cas1 proteins against complex DNA substrates. CRISPR 1311, 251–264.

Bolotin, A., Quinquis, B., Sorokin, A., Ehrlich, S.D., 2005. Clustered regularly interspaced short palindrome repeats (CRISPRs) have spacers of extrachromosomal origin. Microbiology 151 (8), 2551–2561.

Deveau, H., Barrangou, R., Garneau, J.E., Labonté, J., Fremaux, C., Boyaval, P., Romero, D.A., Horvath, P., Moineau, S., 2008. Phage response to CRISPR-encoded resistance in Streptococcus thermophilus. J. Bacteriol. 190 (4), 1390–1400.

Dixit, B., Anand, V., Hussain, M.S., Kumar, M., 2021. The CRISPR-associated Cas4 protein from Leptospira interrogans demonstrate versatile nuclease activity. Curr. Res. Microb. Sci. 2, 100040.

Dixit, B., Ghosh, K.K., Fernandes, G., Kumar, P., Gogoi, P., Kumar, M., 2016. Dual nuclease activity of a Cas2 protein in CRISPR-Cas subtype I-B of Leptospira interrogans. FEBS Lett. 590 (7), 1002–1016.

Dupureur, CM., 2008. Roles of metal ions in nucleases. Curr. Opin. Chem. Biol. 12 (2), 250–255.

Fernandes, L.G.V., Hornsby, R., ALTOd, N., Nally, J., 2021. Genetic manipulation of pathogenic Leptospira: CRISPR interference (CRISPRi)-mediated gene silencing and rapid mutant recovery at 37°C. Sci. Rep. 11 (1), 1–12.

Garneau, J.E., Dupuis, M.È., Villion, M., Romero, D.A., Barrangou, R., Boyaval, P., Fremaux, C., Horvath, P., Magadán, A.H., Moineau, S., 2010. The CRISPR/Cas bacterial immune system cleaves bacteriophage and plasmid DNA. Nature 468 (7320), 67.

Gouet, P., Robert, X., Courcelle, E., 2003. ESPript/ENDscript: extracting and rendering sequence and 3D information from atomic structures of proteins. Nucleic Acids Res. 31 (13), 3320–3323.

Haft, D.H., Selengut, J., Mongodin, E.F., Nelson, KE., 2005. A guild of 45 CRISPR-associated (Cas) protein families and multiple CRISPR/Cas subtypes exist in prokaryotic genomes. PLoS Comput. Biol. 1 (6), e60.

He, Y., Wang, M., Liu, M., Huang, L., Liu, C., Zhang, X., Yi, H., Cheng, A., Zhu, D., Yang, Q., 2018. Cas1 and Cas2 from the type II-C CRISPR-Cas system of Riemerella anatipestifer are required for spacer acquisition. Front. Cell. Infect. Microbiol. 8, 195.

Heler, R., Marraffini, L.A., Bikard, D., 2014. Adapting to new threats: the generation of memory by CRISPR-Cas immune systems. Mol. Microbiol. 93 (1), 1–9.

Holm LRosenstrom P, 2010. Dali server: conservation mapping in 3D. Nucleic Acids Res. 38, W545–W549. Web Server issue.

Yang, J., Li, J., Wang, J., Sheng, G., Wang, M., Zhao, H., Yang, Y., Wang, Y., 2020. Crystal structure of Cas1 in complex with branched DNA. Sci. China Life Sci. 63 (4), 516–528.

Ka, D., Jang, D.M., Han, B.W., Bae, E., 2018. Molecular organization of the type II-A CRISPR adaptation module and its interaction with Cas9 via Csn2. Nucleic Acids Res. 46 (18), 9805–9815.

Ka, D., Lee, H., Jung, Y.D., Kim, K., Seok, C., Suh, N., Bae, E., 2016. Crystal structure of Streptococcus pyogenes Cas1 and its interaction with Csn2 in the type II CRISPR-Cas system. Structure 24 (1), 70–79.

Khrustaleva, TA., 2014. Secondary structure preferences of mn (2+) binding sites in bacterial proteins. Adv. Bioinform. 2014, 501841.

Kieper, S.N., Almendros, C., Behler, J., McKenzie, R.E., Nobrega, F.L., Haagsma, A.C., Vink, J.N., Hess, W.R., Brouns, SJ., 2018. Cas4 facilitates PAM-compatible spacer selection during CRISPR adaptation. Cell Rep. 22 (13), 3377–3384.

Kim, T.Y., Shin, M., Huynh Thi Yen, L., Kim, JS., 2013. Crystal structure of Cas1 from Archaeoglobus fulgidus and characterization of its nucleolytic activity. Biochem. Biophys. Res. Commun. 441 (4), 720–725.

Koonin, E.V., Makarova, K.S., Zhang, F., 2017. Diversity, classification and evolution of CRISPR-Cas systems. Curr. Opin. Microbiol. 37, 67–78.

Kumar, M., Kaur, S., Kariu, T., Yang, X., Bossis, I., Anderson, J.F., Pal, U., 2011. Borrelia burgdorferi BBA52 is a potential target for transmission blocking Lyme disease vaccine. Vaccine 29 (48), 9012–9019.

Lee, H., Zhou, Y., Taylor, D.W., Sashital, DG., 2018. Cas4-dependent prespacer processing ensures high-fidelity programming of CRISPR arrays. Mol. Cell 70 (1), 48–59 e5.

Levy, A., Goren, M.G., Yosef, I., Auster, O., Manor, M., Amitai, G., Edgar, R., Qimron, U., Sorek, R., 2015. CRISPR adaptation biases explain preference for acquisition of foreign DNA. Nature 520 (7548), 505–510.

Li, M., Wang, R., Zhao, D., Xiang, H., 2014. Adaptation of the Haloarcula hispanica CRISPR-Cas system to a purified virus strictly requires a priming process. Nucleic Acids Res. 42 (4), 2483–2492.

Liu, T., Liu, Z., Ye, Q., Pan, S., Wang, X., Li, Y., Peng, W., Liang, Y., She, Q., Peng, N., 2017. Coupling transcriptional activation of CRISPR–Cas system and DNA repair genes by Csa3a in sulfolobus islandicus. Nucleic Acids Res. 45 (15), 8978–8992.

Makarova, K.S., Aravind, L., Grishin, N.V., Rogozin, I.B., Koonin, EV., 2002. A DNA repair system specific for thermophilic Archaea and bacteria predicted by genomic context analysis. Nucleic Acids Res. 30 (2), 482–496.

Makarova, K.S., Grishin, N.V., Shabalina, S.A., Wolf, Y.I., Koonin, EV., 2006. A putative RNA-interference-based immune system in prokaryotes: computational analysis of the predicted enzymatic machinery, functional analogies with eukaryotic RNAi, and hypothetical mechanisms of action. Biol. Direct 1, 7.

Makarova, K.S., Haft, D.H., Barrangou, R., Brouns, S.J., Charpentier, E., Horvath, P., Moineau, S., Mojica, F.J., Wolf, Y.I., Yakunin, AF., 2011. Evolution and classification of the CRISPR–Cas systems. Nat. Rev. Microbiol. 9 (6), 467.

Makarova, K.S., Wolf, Y.I., Alkhnbashi, O.S., Costa, F., Shah, S.A., Saunders, S.J., Barrangou, R., Brouns, S.J., Charpentier, E., Haft, DH., 2015. An updated evolutionary classification of CRISPR–Cas systems. Nat. Rev. Microbiol. 13 (11), 722.

Malmström, J., Beck, M., Schmidt, A., Lange, V., Deutsch, E.W., Aebersold, R., 2009. Proteome-wide cellular protein concentrations of the human pathogen Leptospira interrogans. Nature 460 (7256), 762–765.

Mojica, F.J., Díez-Villaseñor, J., García-Martínez, J., Almendros, C., 2009. Short motif sequences determine the targets of the prokaryotic CRISPR defence system. Microbiology 155 (3), 733–740.

Nuñez, J.K., Harrington, L.B., Kranzusch, P.J., Engelman, A.N., Doudna, J.A., 2015. Foreign DNA capture during CRISPR–Cas adaptive immunity. Nature 527 (7579), 535–538.

Nuñez, J.K., Kranzusch, P.J., Noeske, J., Wright, A.V., Davies, C.W., Doudna, J.A., 2014. Cas1–Cas2 complex formation mediates spacer acquisition during CRISPR–Cas adaptive immunity. Nat. Struct. Mol. Biol. 21 (6), 528–534.

Pourcel, C., Salvignol, G., Vergnaud, G., 2005. CRISPR elements in Yersinia pestis acquire new repeats by preferential uptake of bacteriophage DNA, and provide additional tools for evolutionary studies. Microbiology 151 (3), 653–663.

Prakash, A., Kumar, M., 2021. Characterizing the transcripts of Leptospira CRISPR IB array and its processing with endoribonuclease LinCas6. Int. J. Biol. Macromol. 182, 785–795.

Rollie, C., Graham, S., Rouillon, C., White, M.F., 2018. Prespacer processing and specific integration in a type IA CRISPR system. Nucleic Acids Res. 46 (3), 1007–1020.

Shah, S.A., Erdmann, S., Mojica, F.J., Garrett, R.A., 2013. Protospacer recognition motifs: mixed identities and functional diversity. RNA Biol. 10 (5), 891–899.

Sievers, F., Higgins, D.G., 2014. Clustal Omega, accurate alignment of very large numbers of sequences. Methods Mol. Biol. 1079, 105–116.

Sternberg, S.H., Richter, H., Charpentier, E., Qimron, U., 2016. Adaptation in CRISPR-Cas systems. Mol. Cell 61 (6), 797–808.

Wang, J., Li, J., Zhao, H., Sheng, G., Wang, M., Yin, M., Wang, Y., 2015. Structural and mechanistic basis of PAM-dependent spacer acquisition in CRISPR-Cas systems. Cell 163 (4), 840–853.

Wei, Y., Chesne, M.T., Terns, R.M., Terns, M.P., 2015. Sequences spanning the leader-repeat junction mediate CRISPR adaptation to phage in Streptococcus thermophilus. Nucleic Acids Res. 43 (3), 1749–1758.

Westra, E.R., Swarts, D.C., Staals, R.H., Jore, M.M., Brouns, S.J., van der Oost, J., 2012. The CRISPRs, they are a-changin': how prokaryotes generate adaptive immunity. Annu. Rev. Genet. 46, 311–339.

Wiedenheft, B., Sternberg, S.H., Doudna, JA., 2012. RNA-guided genetic silencing systems in bacteria and archaea. Nature 482 (7385), 331–338.

Wiedenheft, B., Zhou, K., Jinek, M., Coyle, S.M., Ma, W., Doudna, JA., 2009. Structural basis for DNase activity of a conserved protein implicated in CRISPR-mediated genome defense. Structure 17 (6), 904–912.

Wilkinson, M.E., Nakatani, Y., Staals, R.H., Kieper, S.N., Opel-Reading, H.K., McKenzie, R.E., Fineran, P.C., Krause, K.L., 2016. Structural plasticity and *in vivo* activity of Cas1 from the type IF CRISPR–Cas system. Biochem. J. 473 (8), 1063–1072.

Xiao, G., Yi, Y., Che, R., Zhang, Q., Imran, M., Khan, A., Yan, J., Xa, L., 2019. Characterization of CRISPR-Cas systems in Leptospira reveals potential application of CRISPR in genotyping of Leptospira interrogans. APMIS 127 (4), 202–216.

Xiao, Y., Ng, S., Nam, K.H., Ke, A., 2017. How type II CRISPR–Cas establish immunity through Cas1–Cas2-mediated spacer integration. Nature 550 (7674), 137–141.

Yang, W., 2011. Nucleases: diversity of structure, function and mechanism. Q. Rev. Biophys. 44 (1), 1–93.

Yosef, I., Goren, M.G., Qimron, U., 2012. Proteins and DNA elements essential for the CRISPR adaptation process in Escherichia coli. Nucleic Acids Res. 40 (12), 5569–5576.